

# Pulsar timing residual induced by wideband ultralight dark matter with spin 0,1,2

Sichun Sun<sup>2,\*</sup>, Xing-Yu Yang<sup>3,4,†</sup> and Yun-Long Zhang<sup>1,5,6,‡</sup>

<sup>1</sup>National Astronomy Observatories, Chinese Academy of Science, Beijing, 100101, China

<sup>2</sup>School of Physics, Beijing Institute of Technology, Haidian District, Beijing 100081, China

<sup>3</sup>CAS Key Laboratory of Theoretical Physics, Institute of Theoretical Physics, Chinese Academy of Sciences, Beijing 100190, China

<sup>4</sup>School of Physical Sciences, University of Chinese Academy of Sciences, Beijing 100049, China

<sup>5</sup>School of Fundamental Physics and Mathematical Sciences, Hangzhou Institute for Advanced Study, University of Chinese Academy of Sciences, Hangzhou 310024, China

<sup>6</sup>International Center for Theoretical Physics Asia-Pacific, Beijing/Hangzhou, China



(Received 27 January 2022; accepted 16 August 2022; published 8 September 2022)

The coherent oscillation of ultralight dark matter in the mass regime around  $10^{-23}$  eV induces changes in gravitational potential with the frequency in the nanohertz range. This effect is known to produce a monochromatic signal in the pulsar timing residuals. Here we discuss a multifield scenario that produces a wide spectrum of frequencies, such that the ultralight particle oscillation can mimic the pulsar timing signal of stochastic common spectrum process. We discuss how ultralight dark matter with various spins produces such a wide band spectrum on pulsar timing residuals and perform the Bayesian analysis to constrain the parameters. It turns out that the stochastic background detected by NANOGrav can be associated with a wideband ultralight dark matter.

DOI: 10.1103/PhysRevD.106.066006

## I. INTRODUCTION

The pulsar timing array (PTA) observations are sensitive to the gravitational waves of frequencies around the nanohertz range, including EPTA [1], PPTA [2], and NANOGrav [3] experiments. The PTA observations can probe various astrophysical phenomena including gravitational waves from, e.g., supermassive black hole binaries (SMBHs), inflation, cosmic strings, modified gravity, phase transitions etc. [4]. Interestingly, the recent NANOGrav experiment has reported some evidence for a stochastic common-spectrum process after the analysis of 12.5-year dataset [5–7], which has also been supported in the analysis of PPTA and EPTA datasets [8,9].

Significantly, such kind of common spectrum can be interpreted as stochastic gravitational waves background (SGWB) from various sources [10,11]. If the signal is from the stochastic gravitational waves background, then the characteristic strain of gravitational waves  $h_c(f)$  has the amplitude of order  $10^{-15}$  around the frequency  $f_{\text{yr}} \equiv \text{yr}^{-1} \simeq 31.7 \text{ nHz}$ , with an extended frequency spectrum [7]. The correlator of the timing residuals is  $\langle R_a R_b \rangle = \Gamma_{ab} \int df S_c(f)$ , where  $\Gamma_{ab}$  is the overlap

reduction function. The spectral density is  $S_c(f) = \frac{h_c(f)^2}{12\pi^2 f^3}$ . The measured timing residual of the common spectrum in frequency domain is

$$R_c(f) \equiv \sqrt{\frac{S_c(f)}{T_s}} = \frac{1}{\sqrt{3}} \frac{h_c(f)}{2\pi f} \left(\frac{f_s}{f}\right)^{1/2}, \quad (1)$$

where  $T_s$  is the span between the maximum and minimum times of arrival in the pulsar timing array, and  $f_s \equiv 1/T_s$ .

PTA is also sensitive to the nongravitational wave signals, such as the ultralight dark matter through the timing residuals [12–14]. Oscillating ultralight bosons across the cosmic space are interesting dark matter candidates [15–17], which can be either axionlike pseudoscalars or scalar fields such as moduli [18–21]. The ultralight dark photon field (vector) oscillation [22–24], as well as the dark massive graviton oscillation as dark matter from bimetric gravity [25–30], produced during inflation were also proposed.

The ultralight dark matter can be described by a collection of plane waves with energy  $mc^2$  and momentum  $mv$ , with the typical velocity  $v \simeq 10^{-3}c$  in the halo. The de Broglie wavelength is  $\lambda_{\text{dB}} = \frac{2\pi\hbar}{mv} \simeq 4 \text{ kpc} \left(\frac{10^{-23} \text{ eV}}{m}\right) \left(\frac{10^{-3}}{v}\right)$ . Especially, the ultralight dark matter with the mass around  $10^{-23}$  eV, also known as the fuzzy dark matter, was suggested to resolve small-scale problems of the cold

\*sichunssun@bit.edu.cn

†yangxingyu@itp.ac.cn

‡Corresponding author.  
zhangyunlong@nao.cas.cn

collisionless dark matter models [16,17]. However, if the single scalar field accounts for the whole dark matter density in the Galaxy, then these explanations are in tension with the latest Lyman-alpha forest constraints with the mass below  $2 \times 10^{-20}$  eV [31–35]. The bound becomes more stringent if accounting for the quantum pressure [36,37], and can also be affected by considering different self-interactions [38]. For the wideband case with a spread mass spectrum, there have not been systematic studies on the simulation. The constraints on the vector (dark photon)/tensor ultralight cases are not that clear yet in the literature.

Most of the pulsars in the PTA are located around the distances of order kpc from the Earth within a couple of wavelengths. Fuzzy dark matter induces an oscillating pressure with the angular frequency  $\omega_c = 2m$ . The frequency  $f_c = \frac{\omega}{2\pi} \simeq 4.8 \text{ nHz} (\frac{m}{10^{-23} \text{ eV}})$  leads to the oscillation period  $T_c = f_c^{-1} \simeq 6.6 \text{ yr} (\frac{10^{-23} \text{ eV}}{m})$ . As the cosmological timescale is much larger than  $T_c$ , the average value of the pressure is zero, and the field behaves like pressureless cold dark matter. However, here for the PTA observation, the timescale is of several decades and the oscillation in the pressure needs to be considered.

It is noteworthy that the oscillation frequencies of fuzzy dark matter models fall into the sensitive region of PTA observations. It was already proposed earlier that the ultralight boson oscillation has a similar effect as the gravitational wave in the single pulsar timing deviations [12,14,23], although for a single field dark matter candidate with the fixed mass, the signal is monochromatic. String theory naturally gives rise to more than one complex scalar field from compactification. Those stabilized fields can form an extended spectrum [39–41]. For example, if we consider extra dimensions or equivalent discretized theories like clockwork [43,44] or dynamical dark matter [45,46], a spectrum of scalars/vectors/tensors can arise and form a spread mass spectrum. Such a particle spectrum can produce an extended frequency spectrum in timing residuals.

## II. WIDEBAND MASS SPECTRUM

It is reasonable to assume there is more than one scalar/axion field, e.g., the multiscalar/axions scenario from compactification [39]. The mass distribution of a large number of axions is described by random matrix theories. For the multiaxions as inflatons [40,41], the mass distribution satisfies random matrix Marcenko-Pastur law [47]. For the fuzzy dark matter, it can also be realized in string compactification [39,48]. A typical distribution is given by the Marcenko-Pastur relation, the mass scale around  $10^{-23}$  eV is suppressed by the large volume.

We briefly discuss the mass distribution from the random matrix theory here. The mass matrix can be captured by  $M = R^T R$ , where  $R$  is the  $L \times N$  rectangular matrix. Following Marcenko-Pastur law from 1967 [47],

the eigenvalue probability distribution is  $\mathcal{P}(m^2) = \frac{\sqrt{(m^2 - m_-^2)(m_+^2 - m^2)}}{2\pi\beta\delta^2 m^2}$ , for  $m_-^2 \leq m^2 \leq m_+^2$ . Here  $\beta = \frac{N}{L}$ ,  $m_\pm = \delta(1 \pm \sqrt{\beta})$  are the minimum and maximum of the mass regime. The probability density is zero outside this range, and we also have  $\langle m^2 \rangle = \delta^2$ . In more general cases of compactification, one can identify  $\beta$  with the number of (real) axions involved in inflation divided by the total number of moduli chiral multiplets. The value  $\beta$  is rather model dependent. For example, one can refer to [40,41] for a discussion of the N-flation KKLT (Kachru-Kallosh-Linde-Trivedi) model [42]. For the multicomponent fuzzy dark matter, we assume a similar distribution with some generic values of the parameters.

Now we consider a spectrum of ultralight particles described by the multifields model with total number  $N$ , satisfying a distribution  $P(m) = dn/dm$ , and  $\int dm P(m) = 1$ . The axion number in the mass range  $[m, m + dm]$  is  $NP(m)dm$ . Thus, we have  $P(m)dm = \mathcal{P}(m^2)dm^2$ , which leads to  $P(m) = 2m\mathcal{P}(m^2)$ . The Marcenko-Pastur distribution is

$$P_\beta(m) = \frac{m}{\pi\beta\delta^2} \sqrt{\left(1 - \frac{m_-^2}{m^2}\right)\left(\frac{m_+^2}{m^2} - 1\right)}. \quad (2)$$

Besides, as a comparison in the Bayesian analysis, we also consider the Rayleigh distribution

$$P_\sigma(m) = \frac{m}{\sigma^2} e^{-\frac{m^2}{2\sigma^2}}. \quad (3)$$

It is a distribution for nonnegative-valued random variables. In the next section, we will use these distributions for the Bayesian analysis with the observed data.

## A. Fuzzy dark matter

The ultralight scalar dark matter can also be described by the summation of multifields  $\Phi_\phi(\mathbf{x}, t) = \sum_I \phi_I(\mathbf{x}) \cos[m_I t + \theta_I(\mathbf{x})]$ . Their oscillations will induce the perturbations in the metric. We consider the distribution of the multifields with spectral density  $P(m)$ . In continuous limit, the total profile for the fields is  $\Phi_\phi(\mathbf{x}, t) = \int dm P(m) \tilde{\phi}(m) \cos[mt + \theta_m(\mathbf{x})]$ , where  $\theta_m$  is the random phase. It can be considered as the superposition of dark matter waves, which are similar to the stochastic gravitational waves background from the superposition of massive black hole binary systems. The distributions of energy density and pressure are given by  $\tilde{\rho}(m) \simeq \frac{1}{2} m^2 \tilde{\phi}(m)^2 P(m)$  and  $\tilde{p}(m) \simeq -\tilde{\rho}(m) \cos[2(mt + \theta_m)]$ . The total energy density can be written as  $\rho_\phi \equiv \int dm \tilde{\rho}(m) = \int dm \frac{1}{2} m^2 \tilde{\phi}(m)^2 P(m)$ . To extend the spectrum, we can either assume  $\tilde{\phi}(m)^2$  or  $P(m)$  as different distributions. Notice that different forms of  $\tilde{\phi}(m)^2$  also depend on the

thermal history of the Universe, and axion potentials. It is rather model dependent, see, e.g., Ref. [15]. Here we take a convenient choice  $\tilde{\phi}(m)^2 = \frac{2\rho_\phi}{m^2}$ , which leads to  $\tilde{\rho}(m) \simeq \rho_\phi P(m)$  and  $\int dm P(m) = 1$ . We can make the ansatz for the oscillation part of the potential in the frequency space  $\Psi_{\text{osc}}(\mathbf{x}, t) = \int dm \tilde{\Psi}(m) \cos(2mt + 2\theta_m)$ . After considering the Einstein equations, we can reach the differential gravitational potential induced by the differential axions energy density  $d\rho(m)$  in the mass range  $[m, m + dm]$ . We can use the result in [12] directly, and for each mode we have the result from the monochromatic case  $\tilde{\Psi}(m) = \frac{1}{8M_P^2} \frac{\tilde{\rho}(m)}{m^2} = \frac{1}{8M_P^2} \frac{\rho_\phi P(m)}{m^2}$ . Considering  $m = \pi f$  and  $\rho_\phi \equiv \alpha_0 \rho_{\text{DM}}$ , we reach the wideband distribution of the effective characteristic strain

$$h_c^\phi(f) = \frac{\alpha_0}{M_P^2} \frac{\sqrt{3}\rho_{\text{DM}}}{4\pi f} P(\pi f). \quad (4)$$

Other interesting cases include the spin-1 and spin-2 ultralight dark matter, which can also induce signals in the pulsar timing residuals, see, e.g., Refs. [23,29]. One thing to notice is that both spin-1 and -2 ultralight fields are polarized to certain directions and they are known to produce anisotropic signals in pulsar timing residuals. However, for the extended frequency spectrum with multi-fields, we can assume their polarized directions are randomly selected and the average effect is isotropic. Here we generalize the extended spectrum case to the spin-1 and spin-2 fields in this and the following subsection.

## B. Fuzzy dark photon

The dark photon background can produce a directional anisotropic residual signal [23] or be isotropic with a distinct signature in the two pulsar correlation. We can simply extend the spectrum of the trace part of dark photon induced residuals from previous section. The extended spectrum of the characteristic strain is then given by

$$h_c^A(f) = \frac{\alpha_1}{M_P^2} \frac{\sqrt{3}\rho_{\text{DM}}}{12\pi f} P(\pi f), \quad (5)$$

where  $\rho_A \equiv \alpha_1 \rho_{\text{DM}}$  has been used. It is simply 1/3 of the scalar case  $h_c^\phi(f)$ , we will not fit them with the data later. As we discussed already, to produce the isotropic signal, we can look at a model where the polarizations of the vector fields are randomly selected across the space. Then we need to integrate over all polarization angles. To distinguish this isotropic signal from the stochastic gravitational-wave background, we can further look at two pulsar signal correlations, known as the Hellings-Downs curve for the stochastic gravitational wave [49]. One can see more discussions of these different modes and correlation curves in [23,29].

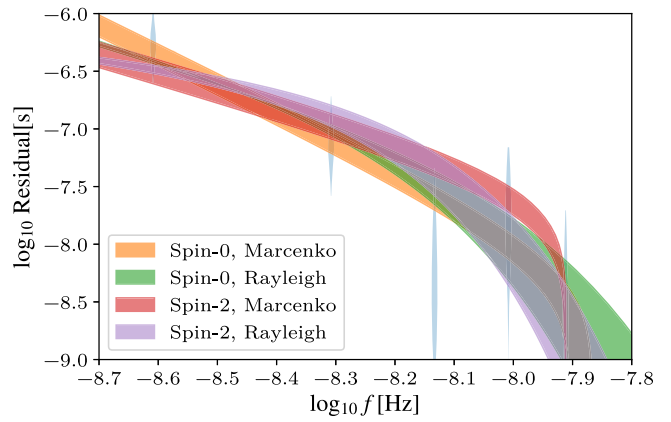


FIG. 1. The timing residuals due to wideband ultralight dark matter in frequency space with different distributions. With the using of Eq. (1), where  $h_c(f)$  is given by Eq. (4) for the spin-0 case, and Eq. (6) for the spin-2 case. The light blue violin points with error bars are reproduced from 12.5 years of NANOGrav data in [7]. The shaded regions indicate one sigma credible intervals. More details of the best fit lines can be found in Fig. 3 in the Appendix.

## C. Fuzzy dark graviton

For the spin-2 ultralight dark matter model construction, one can refer to [27,29] for the bimetric gravity and the Appendix. The local oscillation of such fields with a wideband can then be  $\int dm \mathcal{M}(m) \cos[m t + \theta_m(\mathbf{x})] \varepsilon_{ij} P(m)$ , where  $\theta_m(\mathbf{x})$  is a random phase, and  $\varepsilon_{ij}(\mathbf{x})$  is unit norm, traceless, and symmetric polarization tensor to be averaged over. We also have the total dark matter density as  $\rho_M = \int dm \frac{1}{2} m^2 \mathcal{M}^2 P(m)$ . Take the convenient choice  $\mathcal{M}^2 = \frac{2\rho_M}{m^2}$  and the replacement of  $m \rightarrow 2\pi f$ , we have

$$h_c^M(f) = \frac{\alpha_2}{M_P} \frac{m \mathcal{M} P(m)}{\sqrt{5}} = \frac{\alpha_2}{M_P} \frac{2\sqrt{\rho_M}}{\sqrt{5}} P(2\pi f). \quad (6)$$

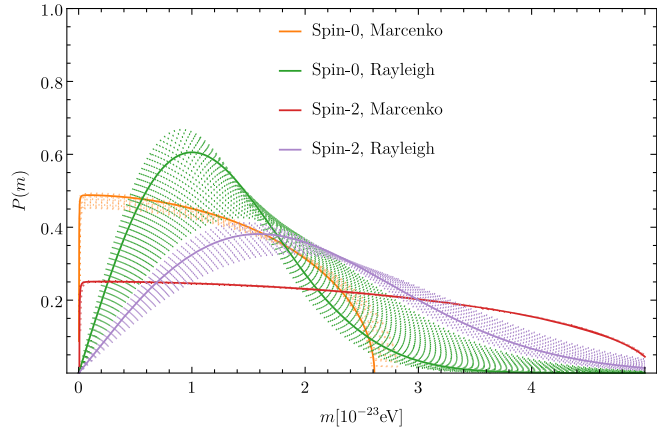


FIG. 2. The probability distribution functions with the best fitting parameters in Table I, as well as the one sigma credible intervals, which are shown by the shaded areas.

TABLE I. The best fitting model parameters with one sigma credible intervals. For the Marcenko-Pastur distribution in Eq. (2), the minimum and maximum of the mass regime  $m_{\pm}^i = \delta_i(1 \pm \sqrt{\beta_i})$  are the derived parameters, the sampled parameters are  $\alpha_i$ ,  $\beta_i$ , and  $\delta_i$ . For the Rayleigh distribution in Eq. (3), the sampled parameters are  $\alpha_i$  and  $\sigma_i$ .

	Parameters	spin-0	spin-1	spin-2
Marcenko	$\alpha_i$	$5.9^{+1.9}_{-1.3}$	$\sim 3\alpha_0$	$7.6^{+2.2}_{-1.7} \times 10^{-7}$
	$m_-^i/(10^{-23} \text{ eV})$	$2.9^{+3.6}_{-0.3} \times 10^{-3}$	$\sim \delta_0(1 - \sqrt{\beta_0})$	$6.3^{+6.0}_{-1.7} \times 10^{-3}$
	$m_+^i/(10^{-23} \text{ eV})$	$2.61^{+0.21}_{-0.01}$	$\sim \delta_0(1 + \sqrt{\beta_0})$	$5.08^{+0.02}_{-0.01}$
Rayleigh	$\alpha_i$	$5.6^{+3.8}_{-1.0}$	$\sim 3\alpha_0$	$6.1^{+2.1}_{-1.3} \times 10^{-7}$
	$\sigma_i/(10^{-23} \text{ eV})$	$1.0^{+0.4}_{-0.1}$	$\sim \sigma_0$	$1.6^{+0.3}_{-0.1}$

Notice here is different from the scalar and vector case where  $m \rightarrow \pi f$ , and  $\rho_M$  will set to be  $\rho_{\text{DM}}$ .

### III. BAYESIAN ANALYSIS

With the Marcenko-Pastur distribution in (2) and Rayleigh distribution in (3), we perform the Bayesian analysis on the first five frequency bins of NANOGrav 12.5-yr dataset [7]. In Fig. 1, we plot the time residuals due to ultralight dark matter with spin-0 and spin-2 in frequency space with different distributions. In Fig. 2, we plot the probability distribution functions with different fitting parameters and distribution functions. The best fitting results are listed in Table I. The one sigma credible intervals are also shown in the figures and table. CMB data and Galaxy surveys have shown the ultralight axions below  $10^{-25} \text{ eV}$  can only compose a small fraction of dark matter [50–57]. For the parameter choice, we consider the mass range for ultralight particles around  $10^{-23} \text{ eV}$  and sample  $\alpha_0, \alpha_2$  as free parameters.

The results in Table I show that if we use the wideband spin-0 model to fit the NANOGrav data, around  $6\rho_{\text{DM}}$  is required. In other words, we can put the constraints of the wideband spin-0 model at this level, which is similar to [14] for the single mass case. Since we consider a wide spectrum of particles, the bounds from Lyman-alpha can be relaxed and it would be interesting to perform a detailed analysis with the observation in the future. In fact, the NANOGrav signals can mainly come from the gravitational waves quadrupolar contribution. In this sense, a small monopole component from scalar dark matter is still possible. For the spin-2 case, due to the tensor structure and multiple modes in (6), the constraints and parameters are different. We can set the whole density as  $\rho_{\text{DM}}$ , and the coupling  $\alpha_2$  is adjustable as in [29]. It would be interesting to perform more detailed data analysis and observational constraints on the spin-2 ultralight dark matter models in future work.

### IV. DISCUSSION

The ultralight dark matter can produce the pulsar timing signals at the monochromatic frequency. Here we generalize it to an extended spectrum, provided a multifeilds

scenario. Then the induced effects are similar to the isotropic stochastic gravitational-wave background in PTA. We also discuss the higher spin cases with vector/dark photon oscillation and spin-2 oscillation. We can see different signals: either with an angular dependence in single pulsar timing residuals as suggested in [23], or isotropic signal with a special curve in two-point timing residuals correlation, provided that the background oscillation polarizations are randomly selected over the galactic scale [58,59]. The later isotropic cases for both spin-1 and spin-2 can mimic the stochastic gravitational-wave background. The ultralight dark matter can also arise from emergent and holographic scenarios [60–64], which would be interesting to study their signals in PTA. For other modes and correlation curves in the metric and pulsar timing array, see, e.g., Refs. [65–70].

In summary, we discuss pulsar timing residuals from the ultralight dark matter oscillation. Especially, we generalize the study with a single frequency to an extended spectrum. Then the ultralight dark matter can also be a viable candidate explaining the claimed common-spectrum at nano-Hz in the NANOGrav 12.5 years dataset. This study provides more interpretations for the NANOGrav results and more means to identify the ultralight dark matter in current and future PTA data. In the future, FAST [71] and SKA [72] can further probe or constrain such wideband ultralight dark matter.

### ACKNOWLEDGMENTS

We thank many valuable suggestions from Professor R.-G. Cai, and helpful discussions with Y. Gao, Z.-K. Guo, J. Liu, S. Pi. This work was supported by the National Natural Science Foundation of China (Grants No. 12005255, No. 12105013, No. 11690022, No. 11821505, No. 11851302, No. 11947302, and No. 11991052), the National Key Research and Development Program of China (Grant No. 2021YFC2201901), the Key Research Program of the Chinese Academy of Sciences (CAS Grant No. XDPB15), the Key Research Program of Frontier Sciences of CAS, and the Fundamental Research Funds for the Central Universities.

## APPENDIX: OSCILLATION INDUCED TIMING RESIDUALS

We review the induced timing residual from single field ultralight dark matter. The ultralight dark matter can be described by the action  $S = \Sigma_{(s)} \int dx^4 \sqrt{-g} \mathcal{L}_{(s)}$ , where  $s = 0, 1, 2$  represent the scalar, vector and tensor fields, respectively. And the energy momentum tensor is given by  $T_{\mu\nu} = \frac{-2}{\sqrt{-g}} \frac{\delta S}{\delta g^{\mu\nu}}$ . The ultralight particle oscillation induces the oscillation of the energy-momentum tensor, so as to trigger the oscillation in the metric. As an approximation, we consider the flat background, with the perturbed metric in the Newtonian gauge

$$ds^2 = -(1 + 2\Phi)dt^2 + [(1 - 2\Psi)\delta_{ij} + h_{ij}]dx^i dx^j. \quad (\text{A1})$$

From the Einstein equations  $G_{\mu\nu} = \frac{1}{M_P^2} T_{\mu\nu}$ , the trace parts of the perturbations lead to

$$-2\nabla^2\Psi = \frac{1}{M_P^2} T^t_t, \quad (\text{A2})$$

$$2\ddot{\Psi} + \frac{2}{3}\nabla^2(\Phi - \Psi) = \frac{1}{3M_P^2} T^k_k, \quad (\text{A3})$$

where the spatial derivatives  $\nabla^2 \equiv \delta^{ij}\partial_i\partial_j$ . The traceless part of the metric perturbation  $h_{ij}$  satisfies

$$\ddot{h}_{ij} - \nabla^2 h_{ij} = \frac{2}{M_P^2} \left( T_{ij} - \frac{1}{3}\delta_{ij}T^k_k \right). \quad (\text{A4})$$

Here we focus on dark matter oscillations across the coherent length at the kpc scale and neglect the cosmic expansion.

### 1. Spin-0: Massive scalar field

We begin with the massive scalar field  $\phi$ , with the Lagrangian density

$$\mathcal{L}_\phi = -\frac{1}{2}(\partial\phi)^2 - \frac{1}{2}m^2\phi^2. \quad (\text{A5})$$

Assuming the profile of the scalar field  $\phi(\mathbf{x}, t) = \phi(\mathbf{x}) \cos [mt + \theta_0(\mathbf{x})]$ , with the random phase  $\theta_0(\mathbf{x})$  and plugging this ansatz into the stress energy tensor. After dropping the subdominant part  $(\nabla\phi)^2 \sim m^2 v^2 \phi^2$ , we obtain the energy density  $\rho_\phi \equiv -T^t_t \simeq \frac{1}{2}m^2\phi^2$ , and pressure  $p_\phi \equiv \frac{1}{3}T^k_k \simeq -\rho_0 \cos [2(mt + \theta_\phi(\mathbf{x}))]$ . This oscillation in the pressure induces the oscillation in the gravitational potentials. In the metric (A1), it is enough to consider the leading oscillating contributions from cosine type  $\Psi \simeq \Psi(\mathbf{x}) + \Psi_\phi \cos [2(mt + \theta_0(\mathbf{x}))]$ , and similarly for  $\Phi$  in the metric (A1). After considering the linearized Einstein equations and  $\rho_\phi = \alpha_0 \rho_{\text{DM}}$ , we can reach

$$\Psi_\phi = \frac{1}{8M_P^2} \frac{\rho_\phi}{m^2} \simeq 6.5 \times 10^{-16} \alpha_0 \left( \frac{10^{-23} \text{ eV}}{m} \right)^2. \quad (\text{A6})$$

For an pulse sent at the point  $\{\mathbf{x}_0, t_0\}$  with frequency  $\omega_0$  and detected at the Earth  $\{\mathbf{x}_\phi, t_\phi\}$  with frequency  $\omega_\phi(t)$ , the Doppler effect leads to

$$z_\phi(t) \equiv \frac{\omega_0 - \omega_\phi(t)}{\omega_0} \simeq \Psi(\mathbf{x}_\phi, t_\phi) - \Psi(\mathbf{x}_0, t_0). \quad (\text{A7})$$

Considering the small velocity  $v \simeq k/\omega \sim 10^{-3}$ , we have neglected higher order terms as discussed in [12]. For the scalar oscillation, the change of frequency can induce the timing residual in the pulse  $R_\phi(t) = \int_0^t z_\phi(t') dt' = \tilde{r}_\phi \cos (2mt + \theta_\phi + \theta_0 - mD)$ , with the amplitude  $\tilde{r}_\phi \equiv \frac{\Psi_\phi}{m} \sin (mD + \theta_\phi - \theta_0)$  and  $D \equiv |\mathbf{x}_\phi - \mathbf{x}_0|$ . The average square value of pulsar-timing residual is

$$\Delta t_\phi = \sqrt{\langle \tilde{r}_\phi \tilde{r}_\phi \rangle} \simeq \frac{1}{\sqrt{2}} \frac{\Psi_\phi}{m} \simeq 30 \text{ ns} \left( \frac{10^{-23} \text{ eV}}{m} \right)^3 \alpha_0. \quad (\text{A8})$$

It is induced by the oscillation of gravitational potential background  $\Psi_\phi$  in (A6).

We can compare this with the timing residuals caused by a monochromatic gravitational wave signal with the strain  $h_\phi$  and amplitude  $\tilde{r}_h = \frac{h_\phi}{\omega} \sin(\frac{\omega D(1-\cos\theta)}{2})(1 + \cos\theta) \sin(2\psi)$  [73,74]. After integrating over  $\theta, \phi, D$ , we have

$$\Delta t_h = \sqrt{\langle \tilde{r}_h \tilde{r}_h \rangle} \simeq \frac{1}{\sqrt{6}} \frac{h_\phi}{\omega}. \quad (\text{A9})$$

The factor of  $\frac{1}{2}$  from Hellings-Downs relation has been considered. We can identify (A8) with (A9). Considering  $\omega = 2m$ , we obtain

$$h_\phi = 2\sqrt{3}\Psi_\phi = \frac{\sqrt{3}}{4M_P^2} \frac{\rho_\phi}{m^2} \simeq 5.2 \times 10^{-17} \alpha_0 \left( \frac{f_{\text{yr}}}{f} \right)^2, \quad (\text{A10})$$

where the frequency  $f = m/\pi$  and  $\rho_\phi = \alpha_0 \rho_{\text{DM}}$  have been considered. Thus, the scalar field dark matter can mimic the monochromatic gravitational wave in PTA. For the spin-1 and spin-2 ultralight dark matter, we briefly summarize the results as below.

### 2. Spin-1: Massive vector field

For the massive vector field  $A_\mu$ , we consider the Lagrangian density

$$\mathcal{L}_A = -\frac{1}{4}F^2 - \frac{1}{4}m^2 A^2. \quad (\text{A11})$$

The oscillating solution of the vector field is given by

$$A_\mu = \mathcal{A}_\mu \cos [mt + \theta_1(x)], \quad (\text{A12})$$

where  $\theta_1(\mathbf{x})$  is a random phase. Such background oscillation can also induce oscillation in the trace part as well as a traceless part in the metric (A1).

For ultralight vector particle, the trace part contributes to the timing residuals, which do not depend on the polarization of the ultralight vector field. Its magnitude is 1/3 of the scalar case, as derived in [23],

$$h_A = \frac{\sqrt{3}}{12M_P^2} \frac{\rho_A}{m^2}. \quad (\text{A13})$$

Thus, the vector field dark matter can also produce the pulsar timing signal at the monochromatic frequency.

For the traceless part of spacial perturbation  $h_{ij}$  in the metric (A1), following the calculation in [23], the photon propagating null geodesic with the perturbed metric is  $\frac{d\xi^\mu}{d\lambda} = -\Gamma_{ab}^\mu \xi^a \xi^b$ . Then we have the modified frequency at the linear level:  $\frac{d\xi^0}{d\lambda} = -\frac{1}{2} \dot{h}_{ij} \omega_0^2 n^i n^j$ , where  $\omega_0$  is the unmodified frequency and  $n^i$  is the unit three-vector. After the integration, we can arrive at

$$z_A(t) \equiv \frac{\omega_0 - w_A(t)}{\omega_0} = \frac{1}{2} n^i n^j [h_{ij}(t_A) - h_{ij}(t_0)]. \quad (\text{A14})$$

For the traceless part, the residual depends on the polarization direction as  $h_A^\theta = \frac{\sqrt{3}}{6M_P^2} (1 + 3 \cos 2\theta) \frac{\rho_A}{m^2}$  [23].

The vector oscillation as discussed in [23] has a preferred direction at each spatial point. It is interesting to discuss whether all the polarization directions aligned or not within a coherent patch. Notice that the current pulsar timing array roughly spans the same length as the ultralight dark matter coherent length at the kpc scale. If vector polarization has a preferred direction, then we can see it from the single pulsar

timing residues, as pointed out in [23]. If the polarization directions for the vector oscillation are stochastic and randomly selected at each point, it is useful to discuss the average isotropic effect. We can then average over the sphere  $(\theta, \phi)$  of all possible directions, and the traceless part above averages to zero.

### 3. Spin-2: Massive tensor field

For a massive spin-2 field  $M_{\mu\nu}$ , according to the dark matter candidate in bimetric gravity [29], we consider the Fierz-Pauli Lagrangian density

$$\mathcal{L}_M = \frac{1}{2} M_{\mu\nu} \mathcal{E}^{\mu\nu\rho\sigma} M_{\rho\sigma} - \frac{1}{4} m^2 (M_{\mu\nu} M^{\mu\nu} - M^2), \quad (\text{A15})$$

where  $\mathcal{E}^{\mu\nu\rho\sigma}$  is the Lichnerowicz operator, which is defined via  $\mathcal{E}_{\rho\sigma}^{\mu\nu} \equiv \delta_\rho^\mu \delta_\sigma^\nu \square - g^{\mu\nu} g_{\rho\sigma} \square + g^{\mu\nu} \nabla_\rho \nabla_\sigma + g_{\rho\sigma} \nabla^\mu \nabla^\nu - \delta_\sigma^\mu \nabla^\nu \nabla_\rho - \delta_\rho^\mu \nabla^\nu \nabla_\sigma$ , and  $M = g^{\mu\nu} M_{\mu\nu}$ . The oscillating solution of the spin-2 field is given by

$$M_{ij} = \mathcal{M} \cos [mt + \theta_2(x)] \varepsilon_{ij}, \quad (\text{A16})$$

where  $\theta_2(\mathbf{x})$  is a random phase, and  $\varepsilon_{ij}$  is a symmetric and traceless polarization matrix with unit norm.

Now if we consider its impact on the pulsar arriving residual, one can refer to the interaction as below.

$$S_{\text{int}} = -\frac{\alpha_2}{2M_P} \int d^4x \sqrt{-\tilde{g}} M_{\mu\nu} T^{\mu\nu}, \quad (\text{A17})$$

where  $\alpha_2$  characterizes the mixing parameter between the spin-2 field and the matter field. The contribution of  $M_{0\mu}$  are in higher order and higher derivative, so we neglect them and work with  $\tilde{g}_{ij} = \delta_{ij} + \frac{\alpha_2}{M_P} M_{ij}$ . For a free photon with unperturbed four-momentum  $\xi^\mu = \omega_0(1, n^i)$ , we have the geodesics  $\frac{d\xi^0}{d\lambda} = -\frac{\alpha_2 \omega_0^2}{2M_P} \dot{M}_{ij} n^i n^j$ , where  $\lambda$  is the affine

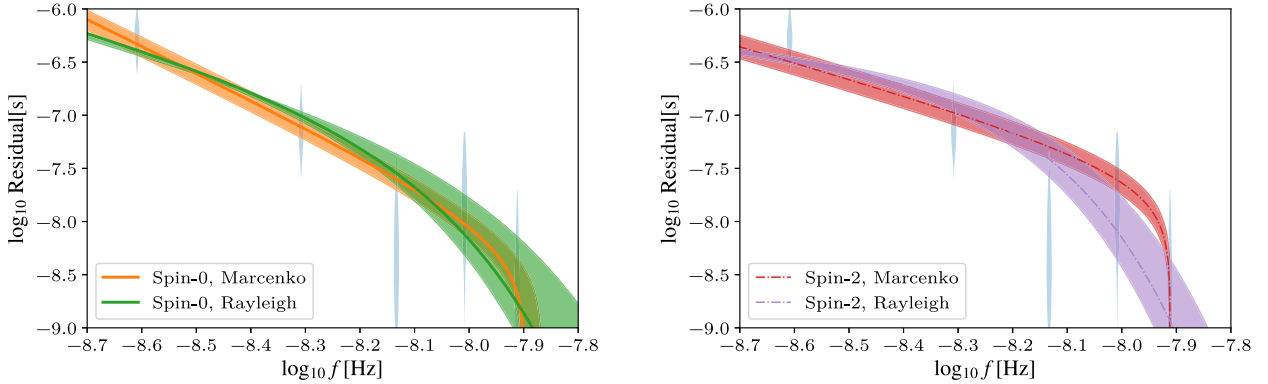


FIG. 3. The timing residuals due to in frequency space with the first five frequency bins of NANOGrav 12.5-yr dataset. Left: the best fit line with one sigma credible intervals of the spin-0 ultralight dark matter with both distributions. Right: the best fit line with one sigma credible intervals of the spin-2 ultralight dark matter with both distributions.

parameter. Then keeping only the linear terms in  $\alpha_2$  and performing the integral, we have

$$z_M(t) \equiv \frac{\omega_0 - w_M(t)}{\omega_0} = \frac{\alpha_2}{2M_P} n^i n^j [M_{ij}(t_M) - M_{ij}(t_0)], \quad (\text{A18})$$

where  $\omega_0$  is the unperturbed frequency at the pulsar.

One can follow the treatment in bimetric gravity, absorb  $M_{\mu\nu}$  in the metric and calculate the delay in the pulses arriving time. For the stochastic background we also need to average over celestial sphere of the spin-2 polarization. The average square value of pulsar-timing residual is

$\Delta t_M \simeq \frac{\alpha_2 \mathcal{M}}{\sqrt{30} M_P} \sin(mt + \theta_2)$  [29]. This corresponds to the gravitational strain

$$h_M = \frac{\alpha_2}{M_P} \frac{\mathcal{M}}{\sqrt{5}} = \frac{\alpha_2}{M_P} \frac{\sqrt{2\rho_M}}{\sqrt{5}m}. \quad (\text{A19})$$

Here  $\rho_M$  can be set as before  $\rho_{\text{DM}} = 0.4 \text{ GeV/cm}^3$ .

More relevant studies on ultralight dark matter can be found in the references [75–115]. In Figs. 4 and 5, we show the results of Bayesian analysis on the first five frequency bins of NANOGrav 12.5-yr dataset for the spin-0 and spin-2 ultralight dark matter with Marcenko-Pastur and distribution, respectively.

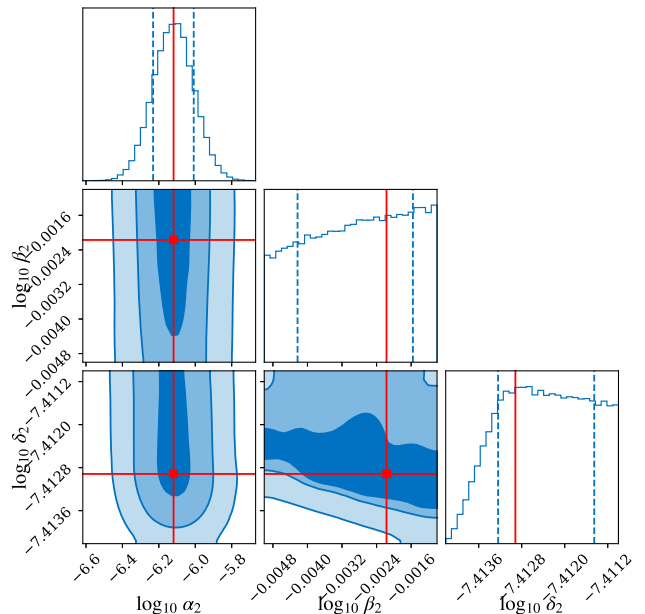
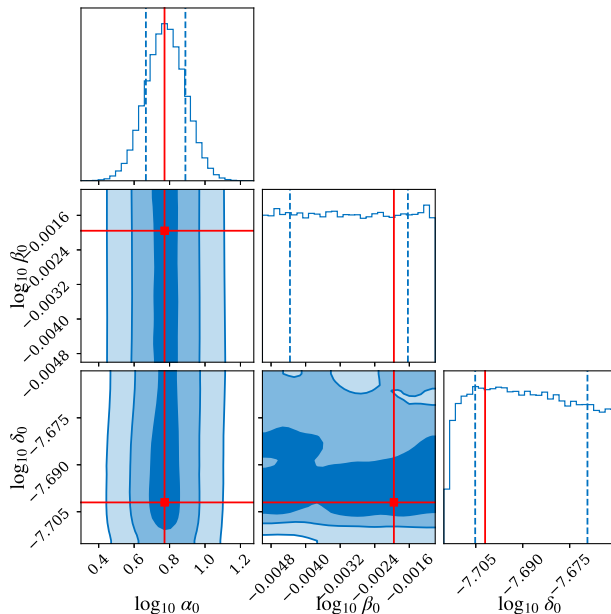


FIG. 4. The Bayesian analysis results on the first five frequency bins of NANOGrav 12.5-yr data for the spin-0 and spin-2 ultralight dark matter with Marcenko-Pastur distribution. Here  $\alpha_i$  and  $\beta_i$  are dimensionless,  $\delta_i$  is plotted with the unit of Hz.

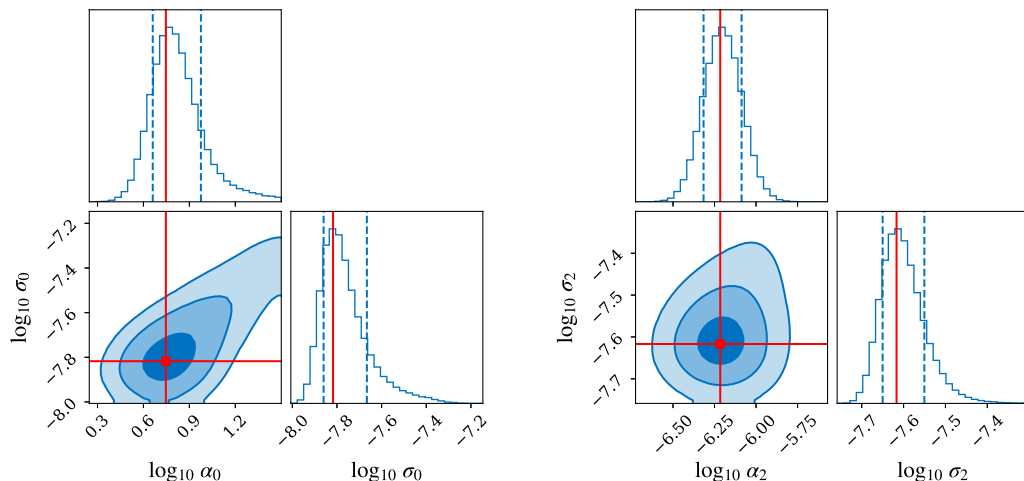


FIG. 5. The Bayesian analysis results on the first five frequency bins of NANOGrav 12.5-yr data for the spin-0 and spin-2 ultralight dark matter with Rayleigh distribution. Here  $\alpha_i$  is dimensionless,  $\sigma_i$  is plotted with the unit of Hz.

- [1] L. Lentati, S. R. Taylor, C. M. F. Mingarelli, A. Sesana, S. A. Sanidas, A. Vecchio, R. N. Caballero, K. J. Lee, R. van Haasteren, S. Babak *et al.*, *Mon. Not. R. Astron. Soc.* **453**, 2577 (2015).
- [2] R. M. Shannon, V. Ravi, L. T. Lentati, P. D. Lasky, G. Hobbs, M. Kerr, R. N. Manchester, W. A. Coles, Y. Levin, M. Bailes *et al.*, *Science* **349**, 1522 (2015).
- [3] Z. Arzoumanian *et al.* (NANOGrav Collaboration), *Astrophys. J.* **859**, 47 (2018).
- [4] M. Anholm, S. Ballmer, J. D. E. Creighton, L. R. Price, and X. Siemens, *Phys. Rev. D* **79**, 084030 (2009).
- [5] M. F. Alam *et al.* (NANOGrav Collaboration), *Astrophys. J. Suppl. Ser.* **252**, 4 (2021).
- [6] M. F. Alam *et al.* (NANOGrav Collaboration), *Astrophys. J. Suppl. Ser.* **252**, 5 (2021).
- [7] Z. Arzoumanian *et al.* (NANOGrav Collaboration), *Astrophys. J. Lett.* **905**, L34 (2020).
- [8] B. Goncharov, R. M. Shannon, D. J. Reardon, G. Hobbs, A. Zic, M. Bailes, M. Curylo, S. Dai, M. Kerr, M. E. Lower *et al.*, *Astrophys. J. Lett.* **917**, L19 (2021).
- [9] S. Chen, R. N. Caballero, Y. J. Guo, A. Chalumeau, K. Liu, G. Shaifullah, K. J. Lee, S. Babak, G. Desvignes, A. Parthasarathy *et al.*, *Mon. Not. R. Astron. Soc.* **508**, 4970 (2021).
- [10] J. Ellis and M. Lewicki, *Phys. Rev. Lett.* **126**, 041304 (2021).
- [11] L. Bian, R. G. Cai, J. Liu, X. Y. Yang, and R. Zhou, *Phys. Rev. D* **103**, L081301 (2021).
- [12] A. Khmelnitsky and V. Rubakov, *J. Cosmol. Astropart. Phys.* **02** (2014) 019.
- [13] N. K. Porayko and K. A. Postnov, *Phys. Rev. D* **90**, 062008 (2014).
- [14] N. K. Porayko, X. Zhu, Y. Levin, L. Hui, G. Hobbs, A. Grudskaya, K. Postnov, M. Bailes, N. D. Ramesh Bhat, W. Coles *et al.*, *Phys. Rev. D* **98**, 102002 (2018).
- [15] P. Arias, D. Cadamuro, M. Goodsell, J. Jaeckel, J. Redondo, and A. Ringwald, *J. Cosmol. Astropart. Phys.* **06** (2012) 013.
- [16] W. Hu, R. Barkana, and A. Gruzinov, *Phys. Rev. Lett.* **85**, 1158 (2000).
- [17] L. Hui, J. P. Ostriker, S. Tremaine, and E. Witten, *Phys. Rev. D* **95**, 043541 (2017).
- [18] J. Preskill, M. B. Wise, and F. Wilczek, *Phys. Lett.* **120B**, 127 (1983).
- [19] L. F. Abbott and P. Sikivie, *Phys. Lett.* **120B**, 133 (1983).
- [20] M. Dine and W. Fischler, *Phys. Lett.* **120B**, 137 (1983).
- [21] P. Svrcek and E. Witten, *J. High Energy Phys.* **06** (2006) 051.
- [22] A. E. Nelson and J. Scholtz, *Phys. Rev. D* **84**, 103501 (2011).
- [23] K. Nomura, A. Ito, and J. Soda, *Eur. Phys. J. C* **80**, 419 (2020).
- [24] B. Salehian, M. A. Gorji, H. Firouzjahi, and S. Mukohyama, *Phys. Rev. D* **103**, 063526 (2021).
- [25] K. Aoki and S. Mukohyama, *Phys. Rev. D* **94**, 024001 (2016).
- [26] E. Babichev, L. Marzola, M. Raidal, A. Schmidt-May, F. Urban, H. Veermae, and M. von Strauss, *Phys. Rev. D* **94**, 084055 (2016).
- [27] L. Marzola, M. Raidal, and F. R. Urban, *Phys. Rev. D* **97**, 024010 (2018).
- [28] J. M. Armaleo, D. López Nacir, and F. R. Urban, *J. Cosmol. Astropart. Phys.* **01** (2020) 053.
- [29] J. M. Armaleo, D. López Nacir, and F. R. Urban, *J. Cosmol. Astropart. Phys.* **09** (2020) 031.
- [30] J. M. Armaleo, D. López Nacir, and F. R. Urban, *J. Cosmol. Astropart. Phys.* **04** (2021) 053.
- [31] V. Iršič, M. Viel, M. G. Haehnelt, J. S. Bolton, and G. D. Becker, *Phys. Rev. Lett.* **119**, 031302 (2017).
- [32] E. Armengaud, N. Palanque-Delabrouille, C. Yèche, D. J. E. Marsh, and J. Baur, *Mon. Not. R. Astron. Soc.* **471**, 4606 (2017).
- [33] T. Kobayashi, R. Murgia, A. De Simone, V. Iršič, and M. Viel, *Phys. Rev. D* **96**, 123514 (2017).
- [34] K. K. Rogers and H. V. Peiris, *Phys. Rev. Lett.* **126**, 071302 (2021).
- [35] L. Hui, *Annu. Rev. Astron. Astrophys.* **59**, 247 (2021).
- [36] J. Zhang, J. L. Kuo, H. Liu, Y. L. S. Tsai, K. Cheung, and M. C. Chu, *Astrophys. J.* **863**, 73 (2018).
- [37] M. Nori, R. Murgia, V. Iršič, M. Baldi, and M. Viel, *Mon. Not. R. Astron. Soc.* **482**, 3227 (2019).
- [38] V. Desjacques, A. Kehagias, and A. Riotto, *Phys. Rev. D* **97**, 023529 (2018).
- [39] M. J. Stott, D. J. E. Marsh, C. Pongkitvanichkul, L. C. Price, and B. S. Acharya, *Phys. Rev. D* **96**, 083510 (2017).
- [40] R. Easter and L. McAllister, *J. Cosmol. Astropart. Phys.* **05** (2006) 018.
- [41] R. G. Cai, B. Hu, and Y. S. Piao, *Phys. Rev. D* **80**, 123505 (2009).
- [42] S. Kachru, R. Kallosh, A. D. Linde and S. P. Trivedi, *Phys. Rev. D* **68**, 046005 (2003).
- [43] D. E. Kaplan and R. Rattazzi, *Phys. Rev. D* **93**, 085007 (2016).
- [44] G. F. Giudice and M. McCullough, *J. High Energy Phys.* **02** (2017) 036.
- [45] K. R. Dienes and B. Thomas, *Phys. Rev. D* **85**, 083523 (2012).
- [46] K. R. Dienes, F. Huang, S. Su, and B. Thomas, *Phys. Rev. D* **95**, 043526 (2017).
- [47] V. A. Marcenko and L. A. Pastur, *Mathematics of the USSR Sbornik* **1**, 457 (1967).
- [48] M. Cicoli, K. Dutta, and A. Maharana, *J. Cosmol. Astropart. Phys.* **08** (2014) 012.
- [49] R. W. Hellings and G. S. Downs, *Astrophys. J. Lett.* **265**, L39 (1983).
- [50] R. Hložek, D. Grin, D. J. E. Marsh, and P. G. Ferreira, *Phys. Rev. D* **91**, 103512 (2015).
- [51] R. Hložek, D. J. E. Marsh, D. Grin, R. Allison, J. Dunkley, and E. Calabrese, *Phys. Rev. D* **95**, 123511 (2017).
- [52] R. Hložek, D. J. E. Marsh, and D. Grin, *Mon. Not. R. Astron. Soc.* **476**, 3063 (2018).
- [53] V. Poulin, T. L. Smith, D. Grin, T. Karwal, and M. Kamionkowski, *Phys. Rev. D* **98**, 083525 (2018).
- [54] A. Laguë, J. R. Bond, R. Hložek, K. K. Rogers, D. J. E. Marsh, and D. Grin, *J. Cosmol. Astropart. Phys.* **01** (2022) 049.
- [55] G. S. Farren, D. Grin, A. H. Jaffe, R. Hložek, and D. J. E. Marsh, *Phys. Rev. D* **105**, 063513 (2022).
- [56] M. Dentler, D. J. E. Marsh, R. Hložek, A. Laguë, K. K. Rogers, and D. Grin, *Mon. Not. R. Astron. Soc.* **515**, stac1946 (2022).

- [57] D. Antypas, A. Banerjee, C. Bartram, M. Baryakhtar, J. Betz, J. J. Bollinger, C. Boutan, D. Bowring, D. Budker, D. Carney *et al.*, arXiv:2203.14915.
- [58] Z. C. Chen, C. Yuan, and Q. G. Huang, *Sci. China Phys. Mech. Astron.* **64**, 120412 (2021).
- [59] Z. Arzoumanian *et al.* (NANOGrav Collaboration), *Astrophys. J. Lett.* **923**, L22 (2021).
- [60] R. G. Cai, S. Sun, and Y. L. Zhang, *J. High Energy Phys.* **10** (2018) 009.
- [61] R. G. Cai, S. Khimphun, B. H. Lee, S. Sun, G. Tumurtushaa, and Y. L. Zhang, *Phys. Dark Universe* **26**, 100387 (2019).
- [62] F. Bigazzi, A. Caddeo, A. L. Cotrone, and A. Paredes, *J. High Energy Phys.* **04** (2021) 094.
- [63] D. Huang, B. H. Lee, G. Tumurtushaa, L. Yin, and Y. L. Zhang, *Phys. Dark Universe* **32**, 100842 (2021).
- [64] S. L. Li, L. Shao, P. Wu, and H. Yu, *Phys. Rev. D* **104**, 043510 (2021).
- [65] I. De Martino, T. Broadhurst, S. H. Henry Tye, T. Chiueh, H. Y. Schive, and R. Lazkoz, *Phys. Rev. Lett.* **119**, 221103 (2017).
- [66] R. Kato and J. Soda, *J. Cosmol. Astropart. Phys.* **09** (2020) 036.
- [67] D. Cyncynates, T. Giurgica-Tiron, O. Simon, and J. O. Thompson, *Phys. Rev. D* **105**, 055005 (2022).
- [68] Y. Chen, M. Jiang, J. Shu, X. Xue, and Y. Zeng, *Phys. Rev. Research* **4**, 033080 (2022).
- [69] M. Demirtas, N. Gendler, C. Long, L. McAllister, and J. Moritz, arXiv:2112.04503.
- [70] X. Xue, Z. Q. Xia, X. Zhu, Y. Zhao, J. Shu, Q. Yuan, N. D. R. Bhat, A. D. Cameron, S. Dai, Y. Feng *et al.*, *Phys. Rev. Research* **4**, L012022 (2022).
- [71] R. Nan, D. Li, C. Jin, Q. Wang, L. Zhu, W. Zhu, H. Zhang, Y. Yue, and L. Qian, *Int. J. Mod. Phys. D* **20**, 989 (2011).
- [72] M. Kramer and B. Stappers, *Proc. Sci.*, AASKA14 (2015) 036.
- [73] F. A. Jenet, A. Lommen, S. L. Larson, and L. Wen, *Astrophys. J.* **606**, 799 (2004).
- [74] Z. L. Wen, F. A. Jenet, D. Yardley, G. B. Hobbs, and R. N. Manchester, *Astrophys. J.* **730**, 29 (2011).
- [75] W. Ratzinger and P. Schwaller, *SciPost Phys.* **10**, 047 (2021).
- [76] C. Xin, C. M. F. Mingarelli, and J. S. Hazboun, *Astrophys. J.* **915**, 97 (2021).
- [77] M. Giovannini, *Eur. Phys. J. C* **82**, 117 (2022).
- [78] S. F. King, S. Pascoli, J. Turner, and Y. L. Zhou, *Phys. Rev. Lett.* **126**, 021802 (2021).
- [79] S. Blasi, V. Brdar, and K. Schmitz, *Phys. Rev. Lett.* **126**, 041305 (2021).
- [80] V. Vaskonen and H. Veermäe, *Phys. Rev. Lett.* **126**, 051303 (2021).
- [81] V. De Luca, G. Franciolini, and A. Riotto, *Phys. Rev. Lett.* **126**, 041303 (2021).
- [82] Y. Nakai, M. Suzuki, F. Takahashi, and M. Yamada, *Phys. Lett. B* **816**, 136238 (2021).
- [83] Y. F. Cai, C. Lin, B. Wang, and S. F. Yan, *Phys. Rev. Lett.* **126**, 071303 (2021).
- [84] A. Addazi, Y. F. Cai, Q. Gan, A. Marciano, and K. Zeng, *Sci. China Phys. Mech. Astron.* **64**, 290411 (2021).
- [85] H. H. Li, G. Ye, and Y. S. Piao, *Phys. Lett. B* **816**, 136211 (2021).
- [86] R. Namba and M. Suzuki, *Phys. Rev. D* **102**, 123527 (2020).
- [87] N. Kitajima, J. Soda, and Y. Urakawa, *Phys. Rev. Lett.* **126**, 121301 (2021).
- [88] G. Domènech and S. Pi, *Sci. China Phys. Mech. Astron.* **65**, 230411 (2022).
- [89] J. Liu, R. G. Cai, and Z. K. Guo, *Phys. Rev. Lett.* **126**, 141303 (2021).
- [90] K. Inomata, M. Kawasaki, K. Mukaida, and T. T. Yanagida, *Phys. Rev. Lett.* **126**, 131301 (2021).
- [91] A. Ashoorioon, A. Rostami, and J. T. Firouzjaee, *Phys. Rev. D* **103**, 123512 (2021).
- [92] N. Ramberg and L. Visinelli, *Phys. Rev. D* **103**, 063031 (2021).
- [93] C. W. Chiang and B. Q. Lu, *J. Cosmol. Astropart. Phys.* **05** (2021) 049.
- [94] M. Gorgetto, E. Hardy, and H. Nicolaescu, *J. Cosmol. Astropart. Phys.* **06** (2021) 034.
- [95] M. Kawasaki and H. Nakatsuka, *J. Cosmol. Astropart. Phys.* **05** (2021) 023.
- [96] S. Nurmi, E. D. Schiappacasse, and T. T. Yanagida, *J. Cosmol. Astropart. Phys.* **09** (2021) 004.
- [97] R. T. Co, K. Harigaya, and A. Pierce, *J. High Energy Phys.* **12** (2021) 099.
- [98] V. S. H. Lee, S. R. Taylor, T. Trickie, and K. M. Zurek, *J. Cosmol. Astropart. Phys.* **08** (2021) 025.
- [99] A. S. Sakharov, Y. N. Eroshenko, and S. G. Rubin, *Phys. Rev. D* **104**, 043005 (2021).
- [100] R. Zambujal Ferreira, A. Notari, O. Pujolàs, and F. Rompineve, *Phys. Rev. Lett.* **128**, 141101 (2022).
- [101] L. Badurina, O. Buchmueller, J. Ellis, M. Lewicki, C. McCabe, and V. Vaskonen, *Phil. Trans. R. Soc. A* **380**, 20210060 (2022).
- [102] Q. Liang and M. Trodden, *Phys. Rev. D* **104**, 084052 (2021).
- [103] R. T. Co, D. Dunsky, N. Fernandez, A. Ghalsasi, L. J. Hall, K. Harigaya, and J. Shelton, arXiv:2108.09299.
- [104] S. D. Odintsov, V. K. Oikonomou, and F. P. Fronimos, *Phys. Dark Universe* **35**, 100950 (2022).
- [105] R. Alves Batista, M. A. Amin, G. Barenboim, N. Bartolo, D. Baumann, A. Bauswein, E. Bellini, D. Benisty, G. Bertone, P. Blasi *et al.*, arXiv:2110.10074.
- [106] Z. Chen, A. Kobakhidze, C. A. J. O'Hare, Z. S. C. Picker, and G. Pierobon, arXiv:2110.11014.
- [107] R. G. Cai, X. Y. Yang, and L. Zhao, arXiv:2109.06865.
- [108] E. Madge, W. Ratzinger, D. Schmitt, and P. Schwaller, *SciPost Phys.* **12**, 171 (2022).
- [109] R. G. Cai, Z. K. Guo, and J. Liu, arXiv:2112.10131.
- [110] M. Khlopov, B. A. Malomed, and I. B. Zeldovich, *Mon. Not. R. Astron. Soc.* **215**, 575 (1985).
- [111] T. Kumar Poddar, S. Mohanty, and S. Jana, *Phys. Rev. D* **101**, 083007 (2020).
- [112] T. Kumar Poddar, S. Mohanty, and S. Jana, *Phys. Rev. D* **100**, 123023 (2019).
- [113] T. K. Poddar, S. Mohanty, and S. Jana, *J. Cosmol. Astropart. Phys.* **03** (2022) 019.
- [114] M. Jain and M. A. Amin, *Phys. Rev. D* **105**, 056019 (2022).
- [115] C. Ferko, G. Satishchandran, and S. Sethi, *Phys. Rev. D* **105**, 024072 (2022).